HHS Public Access

Author manuscript

Adv Biol (Weinh). Author manuscript; available in PMC 2024 December 01.

Published in final edited form as:

Adv Biol (Weinh). 2023 December ; 7(12): e2300157. doi:10.1002/adbi.202300157.

Tetraspanin CD82 associates with trafficking vesicle in muscle cells and binds to dysferlin and myoferlin

Tatiana Fontelonga[1], **Arielle J. Hall**[1], **Jaedon L. Brown**[1], **Youngsook L. Jung**[1], **Matthew S. Alexander**[2,3], **Janice A. Dominov**[4], **Vincent Mouly**[5], **Natassia Vieira**[6], **Mayana Zatz**[7], **Mariz Vainzof**[7], **Emanuela Gussoni**[1,8,*]

[1]Division of Genetics and Genomics, Boston Children's Hospital, MA, USA

[2]Department of Pediatrics, Division of Neurology at Children's of Alabama, University of Alabama at Birmingham, Birmingham, AL, USA

[3]Department of Genetics, University of Alabama at Birmingham, Birmingham, AL, USA

[4]Department of Neurology, University of Massachusetts Worcester, MA, USA

[5]Institute de Myologie/Myology Institute, Paris, FR

[6]Stemcorp, São Paulo, BR

[7]Human Genome and Stem Cells Research Center, Biosciences Institute, University of São Paulo, São Paulo, BR

[8]The Stem Cell Program, Boston Children's Hospital, Boston, MA, USA

Abstract

Tetraspanins organize protein complexes at the cell membrane and are responsible for assembling diverse binding partners in changing cellular states. Tetraspanin CD82 is a useful cell surface marker for prospective isolation of human myogenic progenitors and its expression is decreased in Duchenne muscular dystrophy (DMD) cell lines. The function of CD82 in skeletal muscle remains elusive, partly because the binding partners of this tetraspanin in muscle cells have not been identified. We sought to identify CD82-associated proteins in human myotubes via mass spectrometry proteomics, which identified dysferlin and myoferlin as CD82-binding partners. In human dysferlinopathy (LGMDR2) myogenic cell lines, expression of CD82 protein was near absent in 2 of 4 patient samples. In the cell lines where CD82 protein levels were unaffected, increased expression of the ~72kDa mini-dysferlin product was identified using an antibody recognizing the dysferlin C-terminus. Our data demonstrates that CD82 binds dysferlin/myoferlin in differentiating muscle cells and its expression can be affected by loss of dysferlin in human myogenic cells.

[*]Corresponding author: Emanuela Gussoni, Ph.D, Division of Genetics and Genomics, Boston Children's Hospital, 3 Blackfan Circle, Boston, MA 02115; emanuela.gussoni@enders.tch.harvard.edu.

Conflict of interest statement: None of the authors has any conflict of interest to disclose.

Ethical statement: All authors have read the Journal's position on issues involved in ethical publication and affirm that this report is consistent with those guidelines

Graphical Abstract

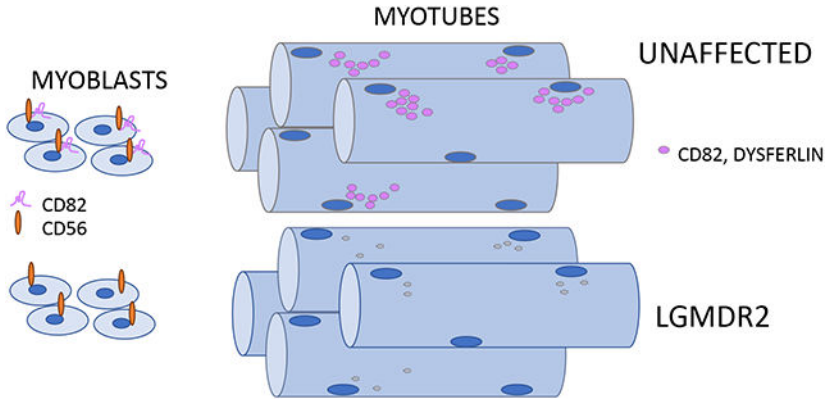

CD82 (purple line) is co-expressed with CD56 (orange) in unaffected myoblasts. In myotubes, CD82 binds both dysferlin and myoferlin and it is co-expressed in vesicles (purple circles). Expression of CD82 is nearly absent in some dysferlinopathy patients, both at the cell surface of myoblasts and in myotubes.

Keywords

Dysferlin; myoferlin; dysferlinopathy; limb girdle muscular dystrophy; Miyoshi myopathy; satellite cell

Introduction

The tetraspanins are a group of transmembrane proteins that participate in a variety of cellular events, including cell shape adaptations, fusion, cellular invasion and cell signaling[1, 2]. Many of these tasks are performed via the assembly of tetraspanin microdomains, where tetraspanins closely associate to signaling proteins or cell adhesion molecules at the cell membrane. Tetraspanins are also located in subcellular membrane vesicles, which include exosomes and endosomal sorting complexes required for transport (ESCRT), thus potentially playing a major role in formation of cargo-containing vesicles as well as vesicle trafficking, both from outside into the cells vice versa from inside out [3, 4]. CD82 was initially discovered as an anti-metastatic tetraspanin whose expression was associated with favorable disease outcomes[5-7]. CD82 is thought to have a typical tetraspanin structure, with short N- and C-termini located intracellularly and two extracellular loops (EC1 and EC2). EC2 is the larger extracellular loop, which is thought to interact with other membrane associated proteins. This EC2 domain is less conserved among tetraspanins, thus often antibodies specific to a given tetraspanin are raised using the EC2 region as an immunogen. Of note, the number of glycosylation sites in the EC2 domain of a given tetraspanin can vary between species. For example, the EC2 domain of human CD82 has 3 known glycosylation sites, while mouse CD82 has 4 sites [8]. Consequently, some antibodies used to prospectively isolate human cells expressing CD82 may not be effective for selection of CD82-expressing cells in the mouse.

Previous work has reported CD82 as essential to maintain quiescence of bone marrow stem cells [9, 10]. In skeletal muscle, CD82 was identified as a good prospective selection marker for human myogenic cells[11, 12]. CD82 was found to bind to integrin alpha7 (ITGA7) in muscle cells and its expression is located at the cell surface of Pax7-positive satellite cells [12]. Ablation of CD82 expression in mice is associated with a mild skeletal muscle phenotype, with increased presence of regenerating myofibers, decreased muscle cell fusion *in vitro* and decreased regeneration potential following acute muscle injury *in vivo* [13]. Importantly, loss of CD82 expression in dystrophin-null mice (mdx^{5cv}), a model for human Duchenne muscular dystrophy [14] displayed an exacerbated phenotype with severe kyphosis, increased intramuscular fibrosis and increased muscle weakness. Increased phosphorylation of mTOR at Ser2448 was observed in the skeletal muscles of dystrophic animals lacking CD82, however the mechanistic link(s) associating loss of CD82 to this severe phenotype are still unknown.

In mature human myotubes, CD82 expression was observed primarily in intracellular vesicles[13], but the exact phenotype of these vesicles was not identified. Different localizations of CD82 during changing cellular states are typical of a tetraspanin and allow it to serve multiple roles by associating with different protein complexes. To gain insight into the function of CD82 in myotubes, we first characterized by immunofluorescence the CD82-labeled vesicles. Strong co-localization of CD82 with caveolae was observed, in addition to partial overlap with Golgi and ER markers. Immunoprecipitations of the CD82 protein complex(es) in human myotubes followed by mass spectrometry were conducted, leading to the identification of new binding partners. These studies revealed potential interactions with dysferlin and myoferlin, which were confirmed by protein co-localizations and immunoprecipitations followed by western blot. Studies on dysferlinopathy patient cell lines demonstrated CD82 expression was completely ablated in 2 of 4 patients. The patients where CD82 expression was ablated carried mutations in the caveolin-binding domain region of dysferlin, and showed decreased or no expression of a previously described ~72 kDa mini-dysferlin [15-17] using antibodies directed to the C-terminus of dysferlin. In contrast, the patients that retained CD82 expression showed robust expression of the ~72 kD mini-dysferlin product. Our data demonstrates the CD82 interactome includes dysferlin and myoferlin and suggests that the 72 kDa mini-dysferlin is potentially implicated in this interaction, thus expanding the functional role of CD82 as a participant in muscle membrane repair.

Methods

Human primary cells and human cell lines.

Human unaffected muscle cells from de-identified, discarded human skeletal muscle were obtained under a protocol approved by the Boston Children’s Hospital IRB. Dysferlinopathy primary muscle cell lines were obtained following patient consent at the University of São Paulo, BR, according to an IRB-approved protocol. Patient J309 is a compound heterozygote for *DYSF* mutation c.952_953del and c.3486_3487del. Total deficiency of dysferlin was observed following muscle biopsy of the bicep. He was seen last in clinic at age 36y and was still able to walk, but had difficulties rising from a sitting position. Patient J322 has

a homozygous *DYSF* pathogenic variant c.2901dupC and on muscle biopsy of the bicep showed a total deficiency of dysferlin protein. He has been non-ambulatory since the age of 28y and his condition can be considered as 'severe'.

Control and dysferlinopathy immortalized cell lines were kindly obtained from the Institut de Myologie cell bank and the information on the lines is publicly available (https://www.jain-foundation.org/scientific-resources/research-tools/cell-lines-dysferlin-research/cell-lines-immortalize). ER (Clone 14; 57.3 divisions) was derived from the quadricep of a 17y old patient with very little dysferlin on muscle biopsy and a homozygous mutation in *DYSF* Exon 44: c.4882G>A. RB (Clone 4; 71.1 divisions) was from a muscle in the forearm of a 43y old patient with dysferlin mutations in Exon 49: c.5497G>T and Exon 49: c.5946+1G>A. Control immortalized lines were named AB 1079 (AB1079C38Q clone 15, 62.0 divisions) from the quadriceps of a 38y old male and AB1190 (Clone 1; 52.4 divisions) from the paravertebral muscle of a 16y old male. Approximately 10^6 live cells per immortalized cell line sample were shipped frozen in 90% Fetal Bovine Serum (FBS) 10% DMSO in dry ice.

Cells were defrosted in a 37°C waterbath and plated on 0.1% gelatin coated plates in proliferation medium, consisting of high glucose (4.5g) DMEM supplemented with 20% FBS, 1% pen/strep and 0.1ng/mL bFGF. To induce myotube formation, cells were switched to differentiation medium, consisting of low glucose DMEM (1g glucose) supplemented with 2%FBS and 1x ITS (insulin, transferrin, selenium GIBCO Thermo Fisher cat# 41400045) for 3-5 days. Cells were maintained in an incubator at 37°C with 5% CO_2.

Immunofluorescence staining on tissue sections

De-identified, discarded adult human skeletal muscle was obtained under a protocol approved by the Boston Children's Hospital IRB. Tissue was frozen in cold isopentane as previously described [18]. Frozen tissue sections were cut at 10μm thickness in a cryostat with the temperature set at −20°C. Unfixed sections were used to co-stain for CD82 and dystrophin; CD82 and CD31. Unfixed sections were immediately blocked in 1xPBS supplemented with 10% fetal bovine serum (FBS) for 45 minutes at RT. Sections were then incubated overnight at 4°C in primary antibody diluted in 1xPBS 5% FBS 0.01% Tween-20. To co-stain for Pax7 and CD82, tissue sections were fixed for 10 min at RT in 4%PFA in PBS. Following a brief rinse in 1xPBS, sections were permeabilized for 3 min at RT in 0.5%Triton X-100 in PBS. Sections were again rinsed briefly in 1XPBS prior to incubation in blocking buffer for 45 min at RT and with primary antibody overnight at 4°C as described above for unfixed sections. Primary antibodies were used at concentrations listed in Supplementary Table 2. Following primary antibody incubation, slides were washed for 3X10 minutes in PBS and incubated with the appropriate secondary antibodies (1:500 Jackson Immunoresearch) and with DAPI (1μg/mL) for 1 hour at room temperature. Slides were washed again in PBS 3X10 minutes in a light protected Coplin jar and then mounted with Vectashield (VectorLabs). Images were captured on a Nikon E1000 Microscope with Visiview Software as previously described[13].

Immunofluorescence staining on cells

Primary human satellite cells were grown on Permanox slides coated with 0.5% gelatin. Cells were expanded for 72 hours in proliferation medium, consisting of high glucose (4.5g) DMEM supplemented with 20% FBS, 1% pen/strep and 0.1ng/mL bFGF. To generate myotubes, cells were switched to differentiation medium, consisting of low glucose (1g) DMEM supplemented with 2%FBS and 1x ITS (insulin, transferrin, selenium supplement) for up to 4 days. For immunofluorescence stainings, cells were then fixed with cold 50:50 methanol:acetone for 2 minutes at −20°C. Slides were blocked for 45 minutes in section block 62711 (Electron Microscopy Sciences). Primary antibodies were used at concentrations listed in Supplementary Table 2 diluted in commercial antibody diluent (Electron Microscopy Sciences) and incubated in a humidified chamber at 4°C overnight. Slides were washed for 3X10 minutes in PBS, incubated with secondary antibodies for 1 hour at room temperature, washed again in PBS 3X10 minutes and then mounted with Vectashield (VectorLabs) with DAPI. Images were captured on a Zeiss AxioImager.Z2 widefield microscope. Images of both myoblasts and myotubes were acquired at 100x magnification, with exposure times remaining consistent within each channel across all images. All images were deconvoluted with Zeiss' Zen Blue imaging software to eliminate noise and improve contrast and were then uploaded into FIJI software (NIH, Bethesda, MD, USA, RRID:SCR_002285) for further processing and analysis. Individual channel images were converted to 8-bit grayscale format and subjected to background subtraction and thresholding to ensure accurate colocalization measurements. Analysis of colocalization between CD82 and the protein of interest was performed using FIJI's integrated Coloc2 plugin, resulting in a Pearson's coefficient for each set of images ranging from −1 to 1, indicating mutual exclusivity or perfect colocalization, respectively. Analyses were performed across 5 or more replicate images for co-localization experiment, after which the average Pearson's coefficient was calculated.

Immunoprecipitations

Human primary muscle cells were purified and cultured as previously described[19, 20]. Upon confluence, cells were differentiated for up to 7 days in DMEM low glucose supplemented with 2% FBS and antibiotics. Total proteins were extracted from 1-2 confluent 15cm plates and lysed in Brij98 lysis buffer (10mM Tris pH 7.4, 1% Brij98, 0.02% NaN_3, 150mM NaCl, 1mM $CaCl_2$, 1mM $MgCl_2$ and protease/phosphatase inhibitors). BCA protein quantification was performed using Pierce™ BCA protein assay kit (Thermo Scientific) and 2X 200µg of lysate were placed in two separate tubes and pre-cleared using 30µl of SureBeads™ Protein G Magnetic beads (BioRad), 1 hour at 4°C. Beads were magnetized using SureBeads™ Magnetic rack (BioRad) and 10µl of input was taken. The remaining lysate from each tube was incubated 3 hours at 4°C, with rotation, in 5µg of anti-CD82 antibody (C33, Sigma) in one tube and mouse gamma globulin (Jackson Immuno) in another tube, as a control. Post incubation, 70µl of SureBeads were added to lysate and incubated, with rotation, overnight at 4°C. Beads were magnetized and lysate discarded. Beads were then boiled at 90°C for 10min in 2X NuPAGE sample buffer (Thermo Scientific) to elute samples.

Mass Spectrometry analyses

100μg immunoprecipitated protein samples were resolved on a 4-20% polyacrylamide gel, stained with Coomassie brilliant blue R-250 (BioRad) and bands excised. Bands were submitted for peptide extraction and sequence to the Harvard Taplin Biological Mass Spectrometry Core Facility. Peptides were entered into an LTQ Orbitrap Velos Pro ion-trap mass spectrometer (Thermo Fisher Scientific, Waltham, MA). Peptide sequences (and hence protein identity) were determined by matching protein databases with the acquired fragmentation pattern by the software program, Sequest [21]. All databases include a reversed version of all the sequences and the data was filtered to between a one and two percent peptide false discovery rate.

Western Blotting

Cells were lysed in RIPA buffer (Boston Bioproducts) supplemented with cOmplete protease inhibitors (Roche). Protein lysates obtained from human cells were sonicated for 3x5 seconds and spun at 13,000 RPM to pellet debris, then the supernatant was collected. Protein concentration was determined using Pierce™ BCA protein assay kit (Thermo Scientific). Samples were made with 4X NUPAGE loading buffer and .05% BME, boiled at 90°C for 10 min and spun at 13,000 RPM, the supernatant was loaded onto a 4-12% Nupage Bis-Tris Gel (Item no, NP0322, Invitrogen) or a 4-20% Tris-Glycine gel (Item no. XP04200, Invitrogen), depending on the target protein to be detected. For confirmatory immunoprecipitations, 10μl of input and 15μg of protein immunoprecipitated with mouse IgG or with anti-human CD82 (C33, Sigma) were run on a 4-20% gel. Protein samples were run at 80V for 10 minutes followed by 115V on ice for 1.5 hours before being transferred to a nitrocellulose or PVDF membrane using a wet transfer. Membranes were blocked for 1 hour at room temperature in 5% non-fat dry milk in TBS-0.1% Tween (TBST) or Odyssey blocking buffer in PBS (LI-COR #927-40000). Primary antibodies (Supplementary Table #2) were diluted as specified and incubated overnight at 4°C. Membranes were washed 3X10 mins with TBST at room temperature, hybridized with an HRP-Conjugated or IRDye 800 (LI-COR #611-132-122) secondary antibody for 1 hour at room temperature, and washed again 3X10 min with TBST. Detection of proteins was determined using Western Lightning ® Plus-ECL Enhanced Chemiluminescence Substrate (Item no. NEL103001EA, Perkin Elmer) and blots were exposed on ProSignal™ Blotting Film (Item no. 30-507L, Prometheus Protein Biology Products, Genesee Scientific). Detection of proteins probed with IRDye 800 was done using the Licor Odyssey 9120 Infrared Imaging System. To ensure equal loading of protein HRP-conjugated blots were stripped using Restore™ Western Blot Stripping Buffer (Item no. 21059, Thermo Scientific) and hybridized with anti-desmin (Item no. ab8592, Abcam), IRDye 800 hybridized blots were normalized with anti-GAPDH polyclonal antibody (Invitrogen #TAB1001). Optical density was measured using FIJI (Image J) Software.

FACS analyses

Primary and immortalized myogenic cell lines were trypsinized and resuspended at a concentration of 1 x 10^7/ml in 5% FBS/HBSS. For each experiment, unstained, CD56 and CD82 single color controls were included. Primary antibodies were added as following: APC anti-CD56 antibody, Clone HCD56 (BioLegend, catalog number: 318310); PE anti-

CD82 antibody, Clone ASL-24 (BioLegend, catalog number: 342103). Antibodies were added to the appropriate cell solutions at a concentration of 5 μl per 1 x 10^6 cells for 20 minutes on ice. Cells were washed and then analyzed using a FACS Aria as previously described[19, 20]. The percentage of single and double-positive cells was determined for each sample following analyses of 10-20K total event counts. Primary cell lines and immortalized cell lines were analyzed by FACS in independent experiments. Gates for CD82 and CD56 positive cells were established based on unstained samples and single-color controls for each experiment.

Statistical Analyses

For the mass spectrometry analyses, the MS/MS pattern matching results against a database were reported at False Discovery Rate (FDR) of 1-2%. Peptide-spectrum match (PSM) was performed by a cross-correlation. PSMs were sorted by their scores. FDR was the ratio between the false PSMs and the total number of PSMs above the score threshold. A Target-Decoy Approach (TDA) was used to estimate an empirical FDR. The FDR values were calculated using the software program, Sequest [21].

Results

Tetraspanins are known to localize to multiple subcellular compartments in living cells and to also change binding partners in different cellular states. We first examined the expression of CD82 in unfixed adult human skeletal muscle tissue sections. CD82 localized at the cell membrane of myofibers (Figure 1A, arrows) and on cells located outside the sarcolemma stained for dystrophin (Figure 1C, open arrowhead). Co-localization of CD82 and the endothelial marker CD31 showed cells co-expressing both markers (Figure 1D, E, arrows). Cells positive for CD82 but negative for CD31 were also noted (Figure 1D-F, filled arrowhead). Co-staining of CD82 and Pax7 revealed that the $CD82^{pos}$ $CD31^{neg}$ cells were satellite cells and CD82 expression was surrounding the cell membrane (Figure 1G-I). A negative control staining was also included (Figure 1J-L), which confirmed signal specificity.

Subcellular localization of CD82 was performed on FACS-sorted human $CD56^+$ $CD82^+$ primary myogenic cells cultured *in vitro*. We previously identified CD82 in intracellular vesicles within differentiating myotubes [13], however the exact identity of these vesicles was not investigated. Immunofluorescence co-staining of CD82 with Golgi, caveolae/lipid rafts, and endoplasmic reticulum markers were conducted in myoblasts (Figure 2) and in myotubes (Supplementary Figure 1). Quantification of co-localization using the Pearson's correlation coefficient indicated the highest co-localization of CD82 with ERGIC in both myoblasts (Figure 2, bottom panels) and myotubes (Supplementary Figure 1, bottom panels). Partial co-localization of CD82 with the Golgi (GOPC) and caveolin 1 or caveolin 3 was also observed, but with a lower Pearson's correlation coefficient compared to ERGIC. Given the broad subcellular localization of CD82 at the membrane and with ER/Golgi vesicles, we sought to identify its binding partners in human myotubes in a non-biased manner, using protein immunoprecipitation followed by mass spectrometry proteomics. Immunoprecipitation of CD82 and its associated proteins was conducted using the anti

C33 antibody, which was previously validated as a CD82-binding antibody [22, 23] using protein lysates from human myotubes. As a negative control, immunoprecipitations using control mouse IgG were conducted in parallel. Immunoprecipitated proteins were run on a gel followed by staining with Coomassie Blue. Bands detected in the CD82-immunoprecipitated lane but not in the IgG control lane were excised and submitted for analysis by mass spectrometry (Figure 3A, arrow). Identified candidates were sorted based on total number of unique peptides and total number of peptides sequenced and 136 proteins were identified as potential CD82 interactors from myotubes (Supplementary Table 1). Among the proteins pulled down with the highest number of total and unique peptides there were MYH9, dysferlin, myoferlin, annexins A1, A2 (ANXA1 and ANXA2), EHD1 and EHD2 [24, 25], which suggested an enrichment for members of the dysferlin complex (Supplementary Table 1; Figure 3B). To validate the potential interaction of these candidates with CD82, co-localization and co-immunoprecipitation experiments were conducted. Co-localization of CD82 and MYH9 in both myoblasts and myotubes indicated a low Pearson's correlation coefficient value in myotubes (0.2-0.3) between CD82 and MYH9 therefore it was not further pursued in the current study. We therefore focused on validating the interaction of CD82 with dysferlin and myoferlin, as these proteins and their associated members, which include MG53 [26, 27], are well-known for their role in muscle fiber repair, myofiber stability and muscle cell differentiation[28-31] We first performed confirmatory immunoprecipitations of CD82 followed by western blots using antibodies to dysferlin (Figure 3C) or myoferlin (Figure 3D). Specificity of the immunoprecipitations was confirmed by presence of the expected bands in the input lanes, while no bands at that size were present in the respective IgG negative control lanes.

With the interaction between CD82 and dysferlin and CD82 and myoferlin confirmed, we next determined in what subcellular entity this interaction was occurring. Dysferlin and myoferlin are known to be expressed at both the myofiber sarcolemma as well as in intracellular vesicles[24, 30, 32]. Human myotubes were co-immunostained with CD82 and a dysferlin specific antibody (Figure 3E, F) or for CD82 and myoferlin (Figure 3G, H). CD82 immunostaining appeared to co-localize with both dysferlin and myoferlin, as confirmed by Pearson's correlation coefficient values of 0.7-0.8 for dysferlin and CD82; or 0.7 for myoferlin and CD82.

Previous work in our lab reported CD82 as a prospective cell surface marker for human myogenic cells[12], thus we next asked whether expression of CD82 in human muscle cells would be affected in dysferlinopathy. We first analyzed by FACS the expression of CD56 and CD82 in human primary myogenic cells from an unaffected individual (Control), a DMD and two dysferlinopathy patients (J309 and J322) (Figure 4A). In the unaffected sample (Figure 4A Control) co-expression of CD56 and CD82 was observed in the upper right quadrant (56.4%), where myogenic cells are expected. In the DMD dystrophic sample (Figure 4A DMD), the percentage of double-positive CD56/CD82 cells was significantly reduced compared to control (13.9%), however CD82 expression was noted in a large percentage of cells that were not expressing CD56 (lower right quadrant 48.3%). In contrast, expression of CD82 at the cell surface was nearly absent in the two dysferlin myoblast samples (J309 and J322), while CD56 expression was observed (33.2% and 8.31%, respectively). To confirm these results, we obtained additional samples of unaffected

and dysferlinopathy patient immortalized cell lines and conducted similar FACS analyses in an independent experiment (Figure 4B). Co-expression of CD56 and CD82 was detected in the samples AB1190 and AB1079 from unaffected individuals (Figure 4B 80.2% and 97.7%, respectively), where myogenic cells are expected. Of the two additional dysferlinopathy cell lines analyzed, RB had a very high percentage of double-positive CD82/CD56 cells and was indistinguishable from control samples, while ER showed robust expression of CD82 in most cells and significantly reduced CD56 expression at the membrane. The difference in CD82 detection at the cell surface between dysferlinopathy patient cell lines led us to investigate whether total CD82 protein was reduced in dysferlin patients via western blot (Figure 4C). It was confirmed that patients J309 and J322 had substantial decrease in CD82 expression, while patients ER and RB did not (Figure 4C). We next used immunofluorescence to assess whether intracellular localization of CD82 in vesicles was affected in the absence of dysferlin in both myoblasts and myotubes from control and patient cell lines. The two normal control cell lines AB1079 and AB1190 showed clear CD82 expression within vesicles (Figure 4D) when compared to the negative control (cells from AB1079 incubated with the secondary antibody only). In dysferlin patient cells, intracellular vesicle localization of CD82 appears indistinguishable from control in the ER cell line, while both J322 and J309 showed much lower levels of CD82 expression (Figure 4D). Thus, the immunofluorescence data supports the findings obtained by FACS and western blot data, demonstrating that CD82 expression can be significantly reduced/absent in some dysferlinopathy patients.

Previous studies have documented that in skeletal muscle both dysferlin and myoferlin are cleaved by calpain 3, generating smaller protein products in the process[15-17]. One of these dysferlin proteolytic products is a 72 kDa isoform that has been shown to accumulate at membrane injury sites when cell repair mechanisms are activated and is detected by antibodies to the C-terminal of dysferlin, but not ones directed to the N-terminal[15, 17]. Muscle cell lysates from control and LGMDR2 patients were analyzed for expression of dysferlin using N- and C-terminal antibodies (Figure 4E, F). With the N-terminal antibody full-length dysferlin protein was detected in the control samples but not in patient samples, including patients ER and RB (Figure 4E). In contrast, with the C-terminal antibody (Hamlet 1) protein bands were detected at the size for full-length dysferlin as well as at ~70 kDa (Figure 4F). Of note, LGMDR2 lysates from patients ER and RB showed robust presence of the 70kDa band, while in comparison J309 and J322 showed decreased expression to near absence, respectively.

Discussion

The tetraspanins are a family of intermembrane proteins known to regulate several different cellular functions from cell shape adaptations to cellular migration[1, 33, 34]. Tetraspanin CD82 is expressed on human satellite cells, it can be used for prospective selection of myogenic progenitors and importantly, its expression is decreased in DMD patient cells[11, 12]. Depletion of CD82 in mice leads to impaired muscle regeneration and its loss in a dystrophic background severely worsens the phenotype leading to weakened muscle force[13]. In the present study, the protein binding partners of CD82 were identified via immunoprecipitations of CD82 in differentiating human myogenic cells. Our data shows

that a protein-protein interaction between dysferlin/myoferlin and CD82 in differentiating myogenic cells occurs.

The ferlin family includes proteins involved in calcium-dependent vesicle fusion, of which dysferlin and myoferlin fall into the Type-I category[15]. Dysferlin mutations result in limb girdle muscular dystrophy 2B (now classified as LGMDR2) and Miyoshi myopathy[29, 35]. In skeletal and heart muscles dysferlin protein is found at the membrane where it anchors via its C-terminus and in cytoplasmic vesicles[30, 32] and it has been implicated in muscle membrane repair, both in isolated myofibers and *in vivo* in mouse models[36, 37]. Dysferlin is expressed at low levels in proliferating myoblasts and its expression increases in differentiating myotubes[28, 38]. Myoferlin has widespread expression in multiple tissues[28, 39] and it is highly upregulated in pre-fusion myoblasts, followed by decreased expression in differentiated myotubes[31]. Myoferlin is essential for myoblast fusion and in its absence myotube formation is severely impaired[24, 25]. Mice lacking myoferlin present with a dystrophic-like phenotype represented by abundant small myofibers and failure to successfully regenerate post-injury[31].

Previous proteomics studies have focused on defining the dysferlin binding partners in both proliferating and differentiating myogenic cells[40]. FLNC, MYH9 and ANXA2, which were pulled down as dysferlin-interacting proteins were also identified in our study as potential CD82-binding proteins, thus supporting the conclusion that CD82 and dysferlin, in myotubes, are part of a larger protein network whose function is still poorly understood. Previous lack of detection of CD82 in these studies [40] as dysferlin-binding protein could be due to different experimental immunoprecipitation conditions, including the differentiation stage of the cells or the type of detergent used to prepare the protein lysates. We found that Briji 98, but not Triton-X, was successful at pulling down proteins associated with CD82 and Briji 98 detergent has been previously used to identify tetraspanin complexes in other cell types [41-43]. Previous studies had documented that loss of dysferlin results in impaired differentiation of myogenic cells via decreased myogenin expression, which implicated HDAC6 and Fam65b as potential partners[44-46]. Our previous work has shown decreased fusion in primary cultures of CD82$^{-/-}$ myoblasts *in vitro* and decreased regeneration *in vivo*[13]. Whether or not this defect is primarily due to loss of CD82 or to a secondary decrease in dysferlin or myoferlin expression in CD82$^{-/-}$ myogenic cells remains to be resolved.

Human patient dysferlinopathy cell lines were used to study whether expression of CD82 in muscle cells is affected by primary mutations in dysferlin. Primary myogenic cells from two patients showed no CD82 expression at the membrane of myoblasts by FACS. These observations were confirmed by western blot using protein lysates from myotubes, and by immunofluorescence detection of CD82 in myotubes. These two patients had mutations towards the N-terminus of the protein, near exons 11, 27 and 31. In contrast, two other patients that showed normal CD82 expression had mutations near the C-terminus of dysferlin, exons 44 and 49. Immunoblots using antibodies to the N-terminus (AbCam) and C-terminus (Hamlet 1) of dysferlin were used to detect cleaved protein products in the patient cell lines. It has been reported that mini-dysferlin arises as a cleavage product from calpain starting from an alternatively spliced exon 40a in dysferlin [15-17]. We

therefore asked if such product might be differentially expressed in the LGMDR2 lines that showed normal expression of CD82 at the membrane, which confirmed the hypothesis. Thus, truncated dysferlin or myoferlin proteins could be sufficient for interaction with CD82 and proper localization of CD82 to the membrane. As to the exact function of this interaction in muscle fibers, additional work will be required to fully elucidate it. While several reports concluded that the 72 kDa mini-dysferlin might be essential for membrane repair and assembly of proteins involved in this process, recent work reported that mice with mutated exon 40a retain membrane repair capacity, thus suggesting a complex regulation of membrane repair via mechanisms that are still not entirely clear [47].

In summary, our study provides evidence of an interaction between dysferlin and myoferlin proteins with tetraspanin CD82 in muscle cells. While the precise function of this interaction is not entirely clear, myogenic cells from some dysferlinopathy patients exhibit a dramatic loss of expression of CD82 at the cell membrane. Our work points to caution and potential limitations for using CD82 as a prospective cell surface marker to isolate primary muscle stem cells from dysferlinopathy patients. Future studies will focus on providing further insight into the significance of these protein interactions, with the goal of better understanding vesicle-mediated membrane repair in dystrophic muscle and how boosting this process might improve myofiber stability in these disorders.

Supplementary Material

Refer to Web version on PubMed Central for supplementary material.

Acknowledgements.

We thank the Hem-Onc HSCI flow cytometry Core Facility at Boston Children's Hospital and the Harvard Taplin Biological Mass Spectrometry Core Facility. We also would like to thank Dr. Mark Scimone and the IDDRC Cellular Imaging Core, funded by NIH P50 HD105351. This work was supported by the National Institutes of Health NIAMS award number 5R01AR069582 (EG). Brazilian patient cell lines were generated under grant CEPID/FAPESP number 2013/08028-1 and CNPr-INCT.

References

1. Termini CM and Gillette JM, Tetraspanins Function as Regulators of Cellular Signaling. Front Cell Dev Biol, 2017. 5: p. 34. [PubMed: 28428953]
2. Hemler ME, Tetraspanin proteins promote multiple cancer stages. Nat Rev Cancer, 2014. 14(1): p. 49–60. [PubMed: 24505619]
3. Perez-Hernandez D., et al. , The intracellular interactome of tetraspanin-enriched microdomains reveals their function as sorting machineries toward exosomes. J Biol Chem, 2013. 288(17): p. 11649–61. [PubMed: 23463506]
4. Andreu Z and Yanez-Mo M, Tetraspanins in extracellular vesicle formation and function. Front Immunol, 2014. 5: p. 442. [PubMed: 25278937]
5. Li W., et al. , A viral microRNA downregulates metastasis suppressor CD82 and induces cell invasion and angiogenesis by activating the c-Met signaling. Oncogene, 2017. 36(38): p. 5407–5420. [PubMed: 28534512]
6. Lee J., et al. , The metastasis suppressor CD82/KAI1 inhibits fibronectin adhesion-induced epithelial-to-mesenchymal transition in prostate cancer cells by repressing the associated integrin signaling. Oncotarget, 2017. 8(1): p. 1641–1654. [PubMed: 27926483]
7. Adachi M., et al. , Correlation of KAI1/CD82 gene expression with good prognosis in patients with non-small cell lung cancer. Cancer Res, 1996. 56(8): p. 1751–5. [PubMed: 8620488]

8. Risinger JI, et al. , Normal viability of Kai1/Cd82 deficient mice. Mol Carcinog, 2014. 53(8): p. 610–24. [PubMed: 23401136]
9. Saito-Reis CA, et al. , The tetraspanin CD82 regulates bone marrow homing and engraftment of hematopoietic stem and progenitor cells. Mol Biol Cell, 2018. 29(24): p. 2946–2958. [PubMed: 30133344]
10. Saito-Reis CA, et al. , Tetraspanin CD82 regulates S1PR1-mediated hematopoietic stem and progenitor cell mobilization. Stem Cell Reports, 2021. 16(10): p. 2422–2431. [PubMed: 34534447]
11. Uezumi A., et al. , Cell-Surface Protein Profiling Identifies Distinctive Markers of Progenitor Cells in Human Skeletal Muscle. Stem Cell Reports, 2016. 7(2): p. 263–78. [PubMed: 27509136]
12. Alexander MS, et al. , CD82 Is a Marker for Prospective Isolation of Human Muscle Satellite Cells and Is Linked to Muscular Dystrophies. Cell Stem Cell, 2016. 19(6): p. 800–807. [PubMed: 27641304]
13. Hall A., et al. , Tetraspanin CD82 is necessary for muscle stem cell activation and supports dystrophic muscle function. Skelet Muscle, 2020. 10(1): p. 34. [PubMed: 33243288]
14. Chapman VM, et al. , Recovery of induced mutations for X chromosome-linked muscular dystrophy in mice. Proc Natl Acad Sci U S A, 1989. 86(4): p. 1292–6. [PubMed: 2919177]
15. Redpath GM, et al. , Calpain cleavage within dysferlin exon 40a releases a synaptotagmin-like module for membrane repair. Mol Biol Cell, 2014. 25(19): p. 3037–48. [PubMed: 25143396]
16. Piper AK, et al. , Enzymatic cleavage of myoferlin releases a dual C2-domain module linked to ERK signalling. Cell Signal, 2017. 33: p. 30–40. [PubMed: 28192161]
17. Lek A., et al. , Calpains, cleaved mini-dysferlinC72, and L-type channels underpin calcium-dependent muscle membrane repair. J Neurosci, 2013. 33(12): p. 5085–94. [PubMed: 23516275]
18. Meng H., et al. , Tissue triage and freezing for models of skeletal muscle disease. J Vis Exp, 2014(89).
19. Spinazzola JM and Gussoni E, Isolation of Primary Human Skeletal Muscle Cells. Bio Protoc, 2017. 7(21).
20. Pakula A, Spinazzola JM, and Gussoni E, Purification of Myogenic Progenitors from Human Muscle Using Fluorescence-Activated Cell Sorting (FACS). Methods Mol Biol, 2019. 1889: p. 1–15. [PubMed: 30367405]
21. Eng JK, McCormack AL, and Yates JR, An approach to correlate tandem mass spectral data of peptides with amino acid sequences in a protein database. J Am Soc Mass Spectrom, 1994. 5(11): p. 976–89. [PubMed: 24226387]
22. Imai T., et al. , C33 antigen recognized by monoclonal antibodies inhibitory to human T cell leukemia virus type 1-induced syncytium formation is a member of a new family of transmembrane proteins including CD9, CD37, CD53, and CD63. J Immunol, 1992. 149(9): p. 2879–86. [PubMed: 1401919]
23. Fukudome K., et al. , Identification of membrane antigen C33 recognized by monoclonal antibodies inhibitory to human T-cell leukemia virus type 1 (HTLV-1)-induced syncytium formation: altered glycosylation of C33 antigen in HTLV-1-positive T cells. J Virol, 1992. 66(3): p. 1394–401. [PubMed: 1738199]
24. Doherty KR, et al. , The endocytic recycling protein EHD2 interacts with myoferlin to regulate myoblast fusion. J Biol Chem, 2008. 283(29): p. 20252–60. [PubMed: 18502764]
25. Posey AD Jr., et al. , Endocytic recycling proteins EHD1 and EHD2 interact with fer-1-like-5 (Fer1L5) and mediate myoblast fusion. J Biol Chem, 2011. 286(9): p. 7379–88. [PubMed: 21177873]
26. Weisleder N., et al. , Recombinant MG53 protein modulates therapeutic cell membrane repair in treatment of muscular dystrophy. Sci Transl Med, 2012. 4(139): p. 139ra85.
27. Zhou L., et al. , Distinct amino acid motifs carrying multiple positive charges regulate membrane targeting of dysferlin and MG53. PLoS One, 2018. 13(8): p. e0202052. [PubMed: 30092031]
28. Posey AD Jr., Demonbreun A, and McNally EM, Ferlin proteins in myoblast fusion and muscle growth. Curr Top Dev Biol, 2011. 96: p. 203–30. [PubMed: 21621072]
29. Liu J., et al. , Dysferlin, a novel skeletal muscle gene, is mutated in Miyoshi myopathy and limb girdle muscular dystrophy. Nat Genet, 1998. 20(1): p. 31–6. [PubMed: 9731526]

30. Lennon NJ, et al. , Dysferlin interacts with annexins A1 and A2 and mediates sarcolemmal wound-healing. J Biol Chem, 2003. 278(50): p. 50466–73. [PubMed: 14506282]
31. Doherty KR, et al. , Normal myoblast fusion requires myoferlin. Development, 2005. 132(24): p. 5565–75. [PubMed: 16280346]
32. Bansal D., et al. , Defective membrane repair in dysferlin-deficient muscular dystrophy. Nature, 2003. 423(6936): p. 168–72. [PubMed: 12736685]
33. Miranti CK, Controlling cell surface dynamics and signaling: how CD82/KAI1 suppresses metastasis. Cell Signal, 2009. 21(2): p. 196–211. [PubMed: 18822372]
34. Hemler ME, Tetraspanin functions and associated microdomains. Nat Rev Mol Cell Biol, 2005. 6(10): p. 801–11. [PubMed: 16314869]
35. Bashir R., et al. , A gene related to Caenorhabditis elegans spermatogenesis factor fer-1 is mutated in limb-girdle muscular dystrophy type 2B. Nat Genet, 1998. 20(1): p. 37–42. [PubMed: 9731527]
36. Roche JA, Lovering RM, and Bloch RJ, Impaired recovery of dysferlin-null skeletal muscle after contraction-induced injury in vivo. Neuroreport, 2008. 19(16): p. 1579–84. [PubMed: 18815587]
37. Cenacchi G., et al. , Ultrastructural changes in dysferlinopathy support defective membrane repair mechanism. J Clin Pathol, 2005. 58(2): p. 190–5. [PubMed: 15677541]
38. Davis DB, et al. , Calcium-sensitive phospholipid binding properties of normal and mutant ferlin C2 domains. J Biol Chem, 2002. 277(25): p. 22883–8. [PubMed: 11959863]
39. Peulen O., et al. , Ferlin Overview: From Membrane to Cancer Biology. Cells, 2019. 8(9).
40. de Morree A., et al. , Proteomic analysis of the dysferlin protein complex unveils its importance for sarcolemmal maintenance and integrity. PLoS One, 2010. 5(11): p. e13854. [PubMed: 21079765]
41. Charrin S., et al. , Differential stability of tetraspanin/tetraspanin interactions: role of palmitoylation. FEBS Lett, 2002. 516(1-3): p. 139–44. [PubMed: 11959120]
42. Rubinstein E., The complexity of tetraspanins. Biochem Soc Trans, 2011. 39(2): p. 501–5. [PubMed: 21428928]
43. Rubinstein E., et al. , CD9, CD63, CD81, and CD82 are components of a surface tetraspan network connected to HLA-DR and VLA integrins. Eur J Immunol, 1996. 26(11): p. 2657–65. [PubMed: 8921952]
44. de Luna N., et al. , Absence of dysferlin alters myogenin expression and delays human muscle differentiation "in vitro". J Biol Chem, 2006. 281(25): p. 17092–17098. [PubMed: 16608842]
45. Ishiba R., et al. , Faster regeneration associated to high expression of Fam65b and Hdac6 in dysferlin-deficient mouse. J Mol Histol, 2019. 50(4): p. 375–387. [PubMed: 31218594]
46. Balasubramanian A., et al. , Fam65b is important for formation of the HDAC6-dysferlin protein complex during myogenic cell differentiation. FASEB J, 2014. 28(7): p. 2955–69. [PubMed: 24687993]
47. Yasa J., et al. , Minimal expression of dysferlin prevents development of dysferlinopathy in dysferlin exon 40a knockout mice. Acta Neuropathol Commun, 2023. 11(1): p. 15. [PubMed: 36653852]

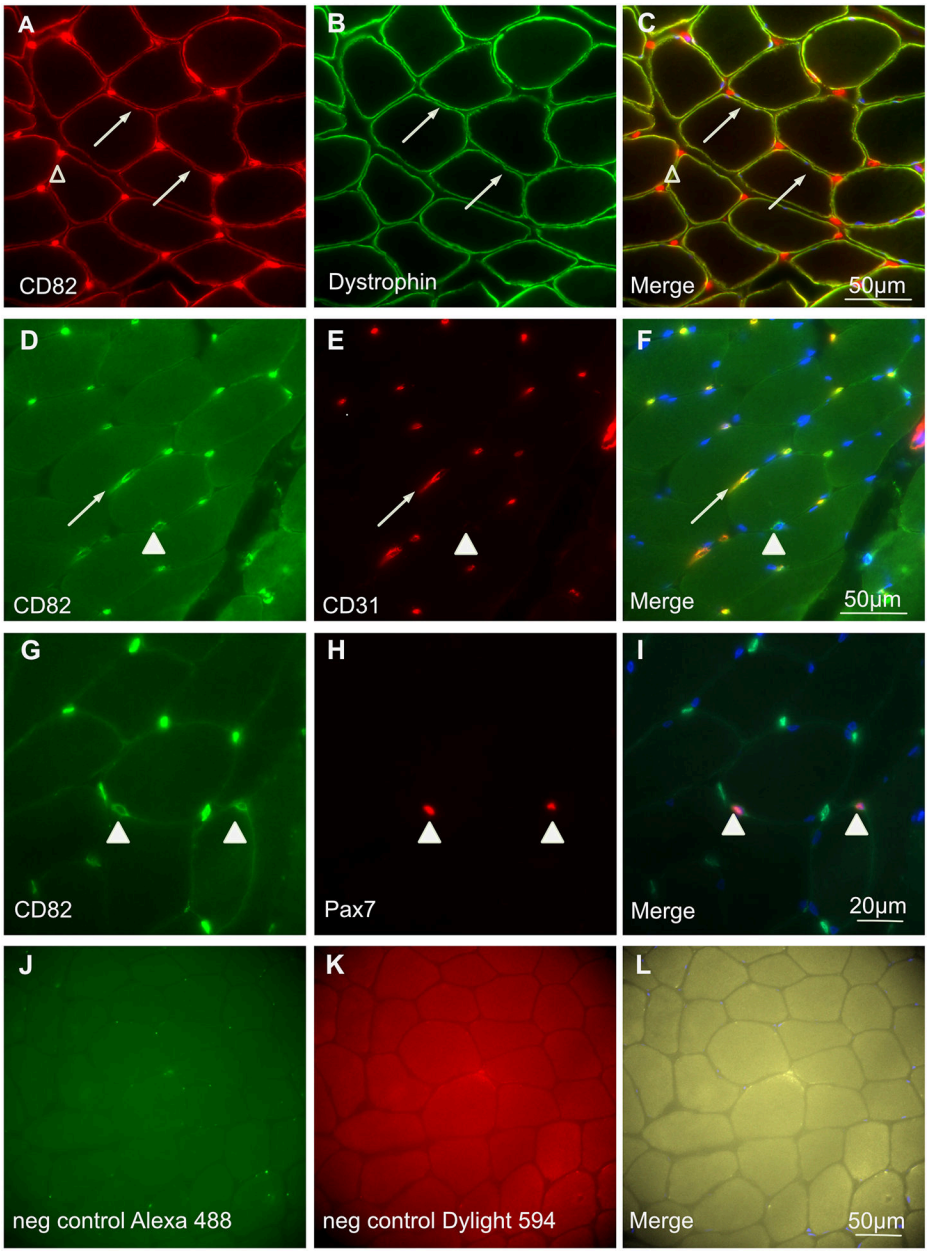

Figure 1. Detection of CD82 expression in human adult skeletal muscle frozen tissue sections.

(A-C) Detection of CD82 at the myofiber membrane of unfixed sections and localizing with dystrophin. CD82 localization at the myofiber membrane is labeled by the arrow, while presumed interstitial cells are marked by an open arrowhead. (D-F) Co-localization of CD82 with CD31 in unfixed tissue sections shows labeling of capillaries and endothelial cells (arrow). Additionally, cells negative for CD31 but positive for CD82 expression were detected (filled arrowhead). (G-I) PFA-fixed tissue sections to co-localize Pax7 and CD82. Co-immunostaining of CD82 (green) and Pax7 (red) shows that CD82 labels the membrane of satellite cells in human muscle tissue sections. The myofiber sarcolemma is also labeled by CD82, but less intensely. J-L. Images of frozen unfixed tissue sections processed in parallel, where the primary antibody was omitted. Images were acquired at high exposure

(using autoexposure), to show lack of signal and confirm specificity of staining when using the primary antibodies. Scale bars are indicated in merged images.

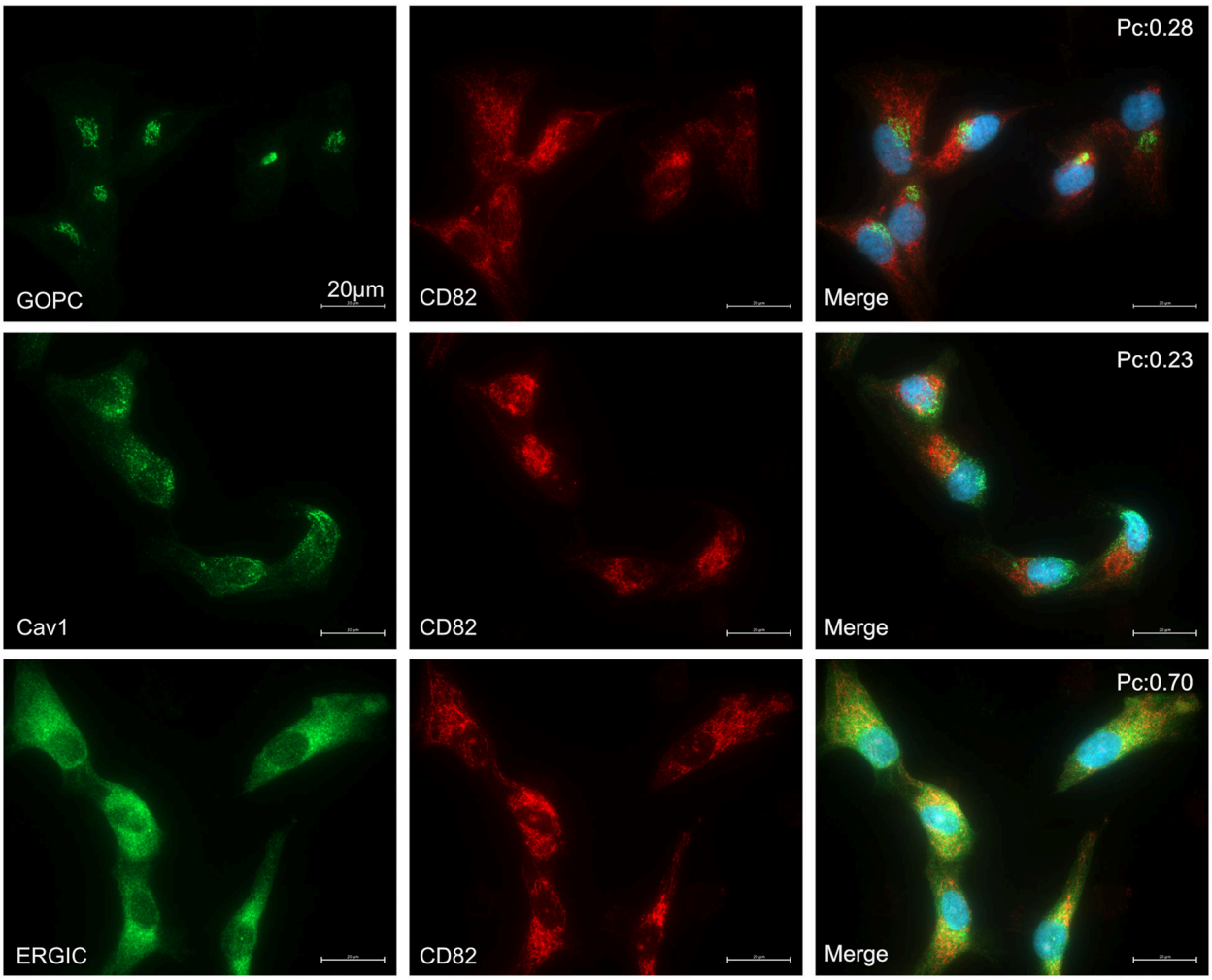

Figure 2. Characterization of CD82 cellular sub-localization in vesicles.

Human primary myogenic cells grown in growth media co stained with the vesicle markers GOPC (Golgi, top panels), caveolin 1 (middle panels) and ER-Golgi intermediate compartment (ERGIC, bottom panels). Images were captured on a Zeiss AxioImager.Z2 widefield microscope at 100x magnification, with exposure times remaining consistent within each channel across all images. Analysis of colocalization between CD82 and the protein of interest was performed using FIJI's integrated Coloc2 plugin. The Pearson's coefficient number (Pc) corresponds to the average number obtained from analysis of 5 or more replicate images for each co-localization experiment. CD82 shows the most predominant co-localization with ERGIC (Pc:0.70). Scale bars=20 μm.

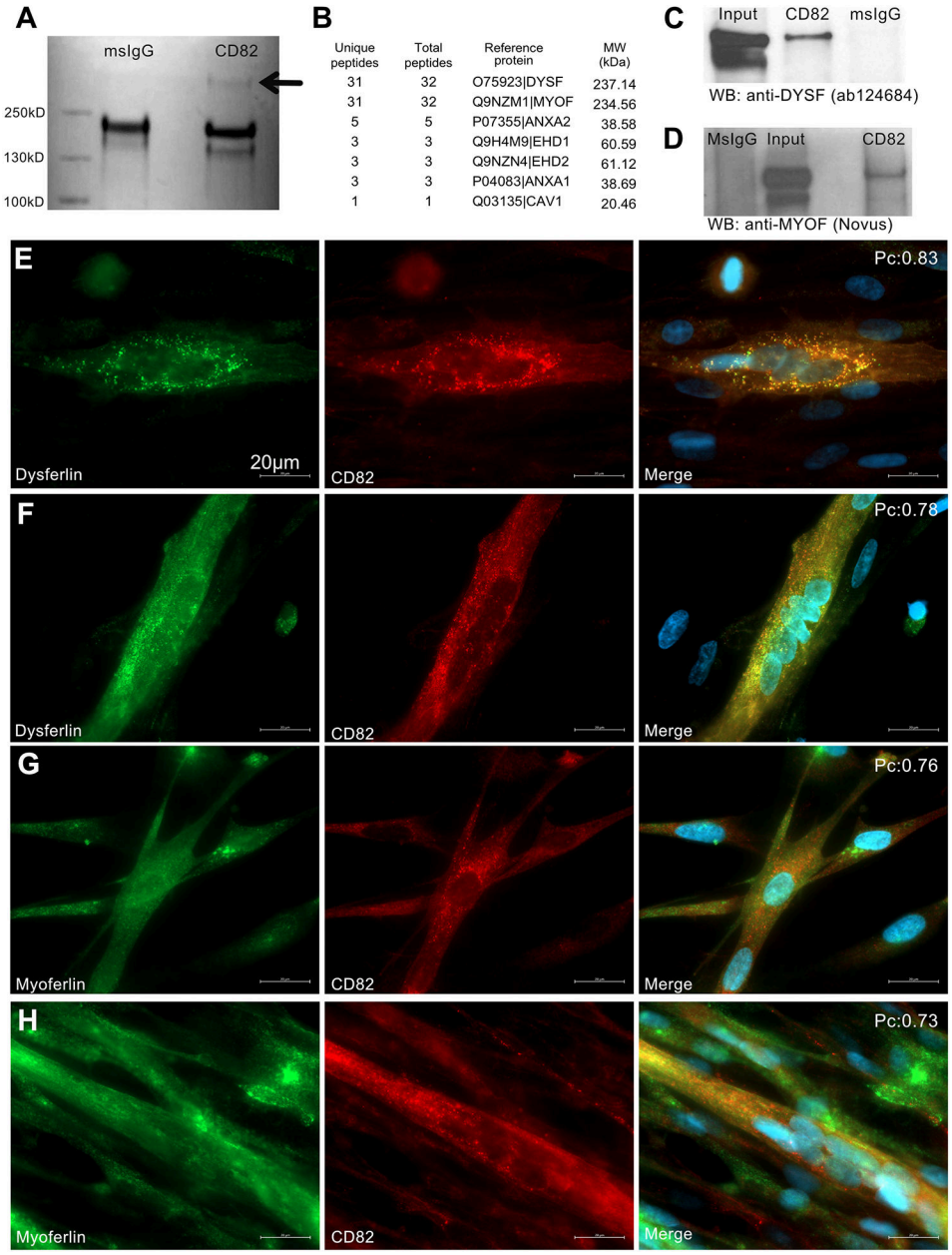

Figure 3. Co-immunoprecipitations and co-localization studies confirm binding of CD82 with dysferlin and myoferlin.

A) Immunoprecipitation of CD82 (IP:CD82) and its associated proteins compared to IgG control run on a gel stained with Comassie blue stain. The gel reveals a ~250 kDa band (black arrow) that was excised and submitted to mass spec analysis. B) Proteins identified by mass spec analysis that are known interactors of dysferlin. C, D) Confirmatory immunoprecipitations followed by western blot to validate interaction between CD82, dysferlin and myoferlin in human myotubes. Dysferlin and myoferlin were pulled down using anti-CD82, while no bands were seen in the control IgG pulldown. E, F) Colocalization of CD82 (Proteintech primary antibody) with dysferlin (AbCam primary Antibody) in human myotubes. The images show co-localization of CD82 and dysferlin

in vesicles and the Pearson's coefficient number (Pc) is shown for each image. G,H) Co-localization of CD82 (Proteintech primary antibody) with myoferlin (AbCam primary antibody). Again, the Pearson's coefficient number (Pc) is shown for each image. Scale bars:=20μm.

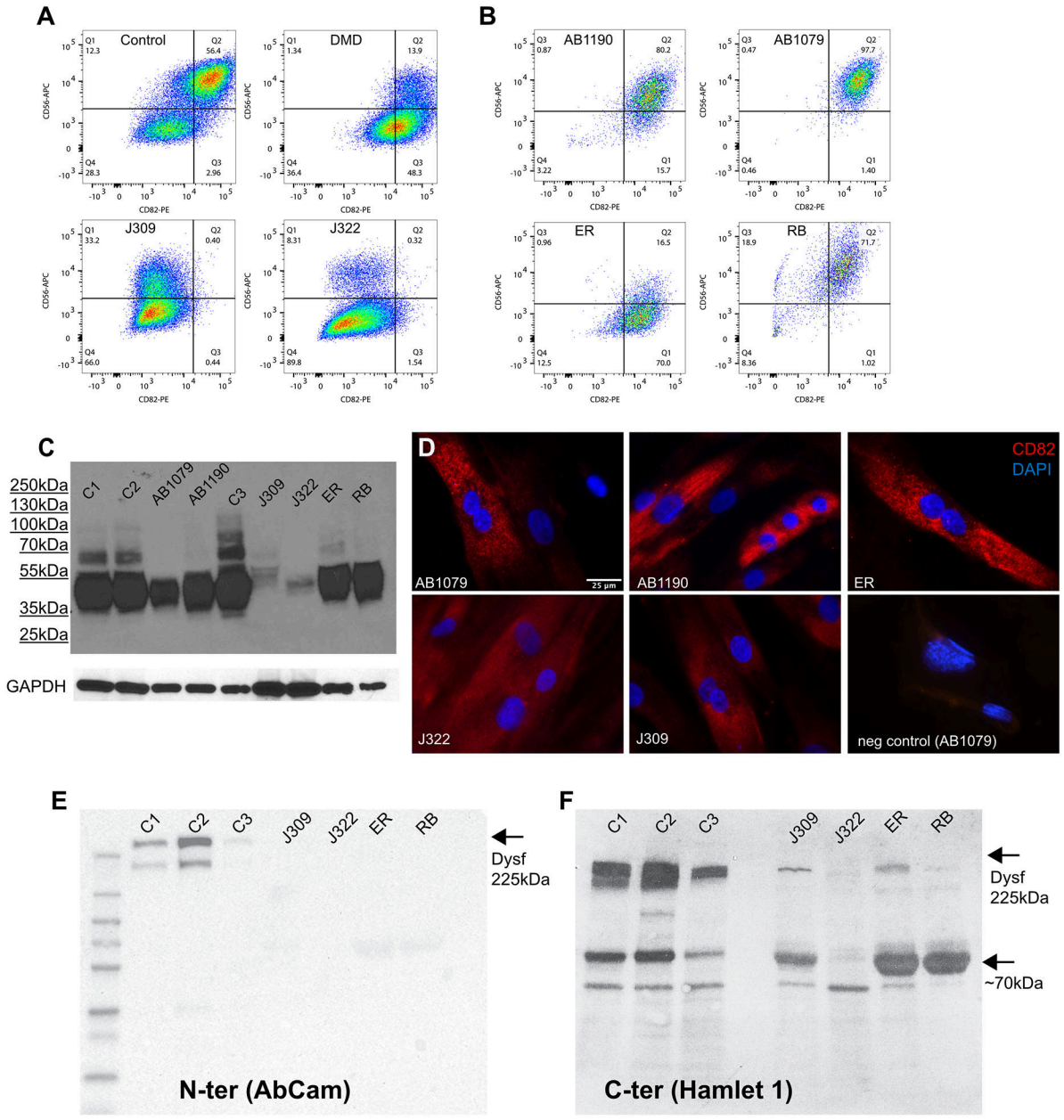

Figure 4. Loss of CD82 expression at the cell membrane in some LGMD2R cell lines.

A, B) FACS plots of primary (A) and immortalized (B) human cell lines to detect expression of CD56 and CD82 in myogenic cells. FACS in A and B were performed independently and gates were established for each experiment based on negative and positive single-color controls. In unaffected control cells (Control; AB1190; AB1079) co-expression of the myogenic markers CD56 (Y axis) and CD82 (X-axis) occurs in the majority of the cells. In LGMDR2 patients J309 and J322, no expression of CD82 is detected, while a variable percentage of myogenic cells is positive for CD56. LGMDR2 patient ER cells show expression of CD82 but loss of CD56, while patient RB shows an expression profile similar to a normal control. C) Western blot expression analysis of CD82 on the same human cell lines confirms the FACS data. D) immunofluorescence detection of CD82 in control

and LGMDR2 cell lines shows expression in vesicles. Again, J322 and J309 cells show severely reduced to near absence of CD82 expression. E) Western blot using an antibody that detects the N-terminus of dysferlin (AbCam) confirms absence of dysferlin expression in all LGMDR2 lines. F) Western blot on the same cell lines as in E using an antibody directed to the C-terminus of dysferlin (Hamlet 1) detected a ~72 kDa product in control, J309, ER and RB lines but not J322.